

# Astronomical Forcing in Cosmogenic Be-10 Variation from East Antarctica Coast?

I. Liritzis and E. Grigori

Research Center for Astronomy and Applied Mathematics  
Academy of Athens  
14 Anagnostopoulou Street,  
Athens 106 73, Greece

## ABSTRACT

LIRITZIS, I. and GRIGORI, E., 1998. Astronomical forcing in cosmogenic Be-10 variation from east Antarctica coast? *Journal of Coastal Research*, 14(3), 1065-1073. Royal Palm Beach (Florida), ISSN 0749-0208.

Cosmogenic  $^{10}\text{Be}$  concentrations in Antarctic ice (Vostok site), during the past 150 ka (1 ka = 1000 years) have been spectrally analyzed. The current interest in beryllium refers on its use as a dating tool in lake, offshore/marine, and ice-core environments, and for palaeoclimate variation and reconstruction. The methods of fast fourier transform, maximum entropy, and power spectrum employing the Blackman-Tukey window, as well as significance tests ( $\chi^2$ , Kolmogorov-Smirnov, analysis per subset, randomness test *etc.*) were applied.

Significant and strongly stationary periodicities centered around 100 ka (large uncertainty, near the record length), 40 ka, 25 ka, 19 ka, 12 ka and 5 ka were found, superimposed upon each other forming a network of periodic cycles. Similar periodicities were previously reported for  $\delta^{18}\text{O}$  variation from V28-239 pacific ocean deep-sea core and other direct or proxy palaeoclimatic data. They are recognized with the well known astronomical frequencies; the long-term variations in the geometry of the earth's orbit and rotation as the fundamental causes of Pleistocene ice-ages of the past 3 Ma. This astronomical forcing (referred to as the Milankovich theory) is for first time observed in  $^{10}\text{Be}$  variation, and interesting observations can be made regarding the contiguity between  $^{10}\text{Be}$  production-deposition rates, palaeoclimate, solar activity, earth's orbit and rotation, sea-level changes and geomagnetic field.

**ADDITIONAL INDEX WORDS:** *Beryllium-10, palaeoclimates, oxygen-18, Milankovich, periodicities.*



## INTRODUCTION

Beryllium-10 (half-life = 1.5 Ma and  $\lambda = 0.462 \times 10^{-6}$  year $^{-1}$ ) is produced by spallation of nitrogen and oxygen atoms by cosmic-rays in the upper atmosphere. Its production rate is proportional to the flux of cosmic rays, which is modulated by solar activity and the strength of the Earth's magnetic field (LAL and PETERS, 1967; LAL, 1987; McHARGUE and DAMON, 1991). In general, beryllium is produced in a manner similar to that of radiocarbon. Be-10 is deposited not only from rain and wind onto land and marine sediments, but also from snow onto mountainous and polar regions. Ice is a good reservoir for  $^{10}\text{Be}$  studies because of a continuous record, good time resolution, independent chronology and minimum interference from other effects.

The  $^{10}\text{Be}$  profile confirms the trends of oxygen isotope curve using the time-scale adopted by (LORIUS *et al.*, 1985).

Studies of the cosmogenic radionuclide  $^{10}\text{Be}$  has generated much interest because of its potential as a tracer in the environment and applications to geochronology, geology, archaeology, glaciology, geophysics, oceanography and astronomy. Therefore, such studies are useful to coastal researchers regarding important new information provided on climate reconstruction, chronostratigraphy, chronological connections between polar and lower latitude climatological records, to mention a few.

Along such reason and due to its importance, the spectral analysis of  $^{10}\text{Be}$  concentration offers a fundamental tool for testing the astronomical theory of climate forcing, which during the last twenty years has gained much respect (BERGER, 1989; BERGER and PESTIAUX, 1984). Moreover, this study provides a new insight of the orbital influence on the periodic sediment accumulation and periodic variation of proxy palaeoclimatic data, offering possible correlations between certain solar-planetary-terrestrial records.

In our present effort, the search for possible periodic variation of  $^{10}\text{Be}$  in glacial deposits focus in particular on the identification of these periodicities with certain other phenomena of terrestrial or astronomical origin, and the subsequent causal interpretation of  $^{10}\text{Be}$  production-transportation-deposition processes.

Although comparison between radiocarbon variations in tree-ring and  $^{10}\text{Be}$  in ice cores have shown excellent correlation for short-term variations (believed to reflect with a high probability production rate variations), interpretation of long-term trends is more problematic. However, correlation with  $\delta^{18}\text{O}$  eases the interpretation of such long-term variation. Indeed, for the Vostok isotopic studies of east Antarctica, the observed  $\delta^{18}\text{O}$ -temperature relationship is quite linear, and the temperature reconstruction is reinforced by the good agreement between accumulation changes derived by transforming the  $\delta^{18}\text{O}$  profile into a temperature profile and those derived from the presently analysed  $^{10}\text{Be}$ .

Obviously, correlations between beryllium, carbon dioxide

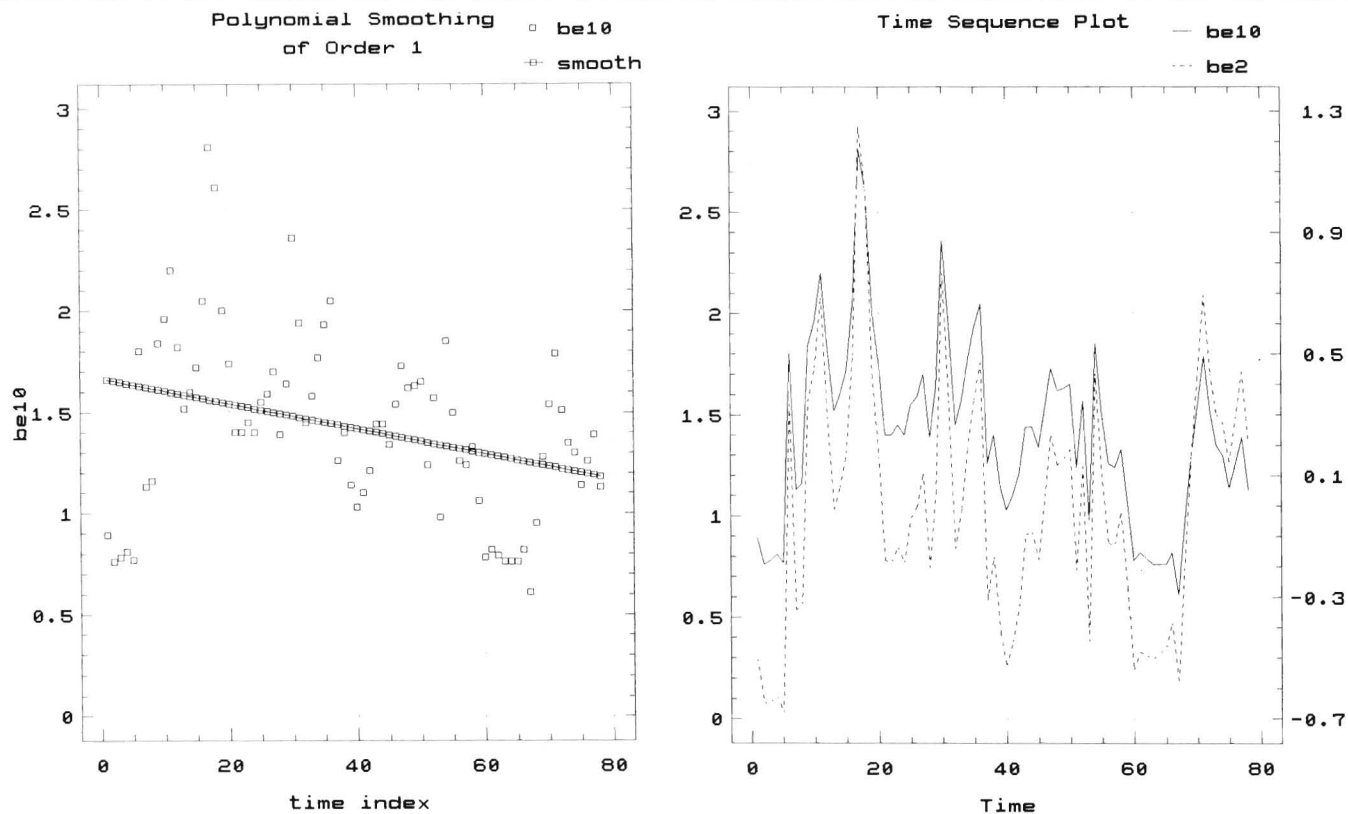


Figure 1. (a)  $^{10}\text{Be}$  concentration ( $\times 10^5$  atoms/g) (dashed) and 1st order polynomial fit (solid) against time, per 2 ka. (b) analyzed residuals of  $^{10}\text{Be}$  after subtraction of the first order polynomial (solid line) and original  $^{10}\text{Be}$  data (dashed line).

(C-14), and other stable isotope profiles in the same ice core enables not only the influence of solar variability on climate to be tasted, but also reflects changes in ice caps and consequently determines rates of rise in sea-level (BOWEN, 1991).

A unique record of  $^{10}\text{Be}$  variations in Vostok and Dome C cores from Antarctica (RAISBECK *et al.*, 1981; 1987), two coastal sites in the Wilkes land, near the coast of C. Hoadley ( $78^\circ 28' \text{ S}$ ,  $106^\circ 48' \text{ E}$ ), covering the past 150 ka has been spectrally analyzed. The long 2,083 m depth ice core was drilled through the ice sheet covering the last glaciation back to  $\sim 150$  ka. Sampling of ice for isotope analysis was done by cutting a continuous slice from the length of the ice after cleaning. Sampling was performed on average every 25 m. The one standard deviation to the measurement uncertainty was less than 3% and the instrumental estimated error was 5%. Multiple measurements for some samples subdivided were made to obtain some information on short-term fluctuations in the  $^{10}\text{Be}$ . The concentrations in the sub-samples agree to within 10% of that for the mean concentration at that level. Maximum and minimum values of 2.81 and  $0.61 \times 10^5$  atoms/g were recorded for number of data,  $N = 78$ , average value = 1.42, stand. dev. = 0.44; while the frequency histogram for the number of  $^{10}\text{Be}$  follows a normal (Gaussian) distribution.

## SPECTRUM ANALYSIS METHODS AND RESULTS

In the time domain autocorrelation was employed, where the intrinsic non-stationarity of the record is emphasized primarily through the variable amplitudes of spectral peaks. The autocorrelation retains all frequency components essentially gathered in the function. Moreover, the lack of spectral resolution is traded for increased time resolution and the ability to detect not only periodicities but also aperiodic transients.

In the frequency domain, three different power spectral analysis techniques have been used: the maximum entropy spectrum analysis (MESA), the fast fourier transform (FFT), and the Blackman-Tukey smoothed spectrum analysis (PSA) attaching significance levels. Tests of significance (*i.e.* the Kolmogorov-Smirnov and randomness tests) and stationarity (analysis of subsets, use of various autoregressive orders, F) were applied (XANTHAKIS *et al.*, 1991; 1995; LIRITZIS *et al.*, 1995; ULRYCH and BISHOP, 1975; CHATFIELD, 1984).

FFT always gives the total length of the record and its various sub-harmonics as the high peak. This also defines periods higher than the length of the time-series.

MESA assumes that the resultant spectrum estimate will be based on all the information in the actual record and will use the least amount of information about the series outside

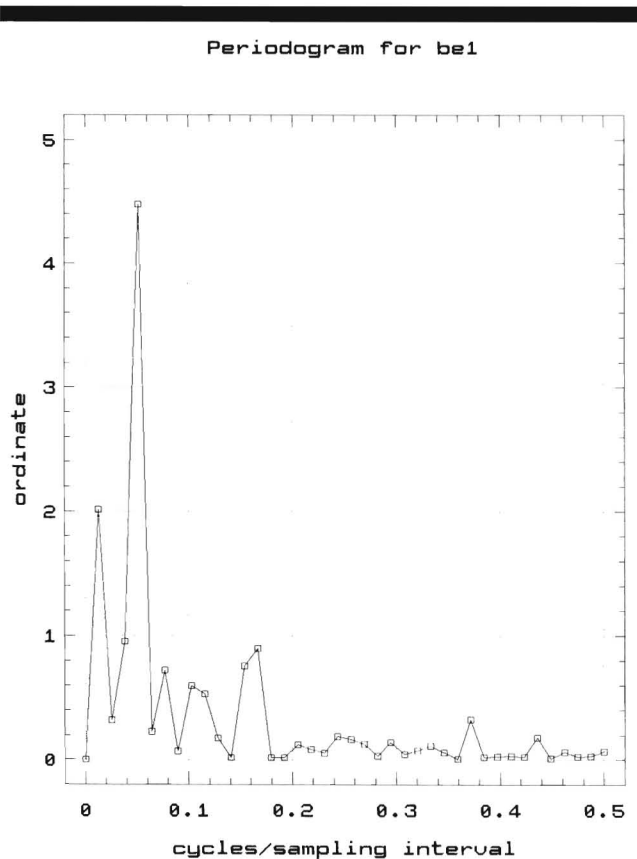


Figure 2. FFT spectrum of all the record. Note the six periodicities presented in Table 1.

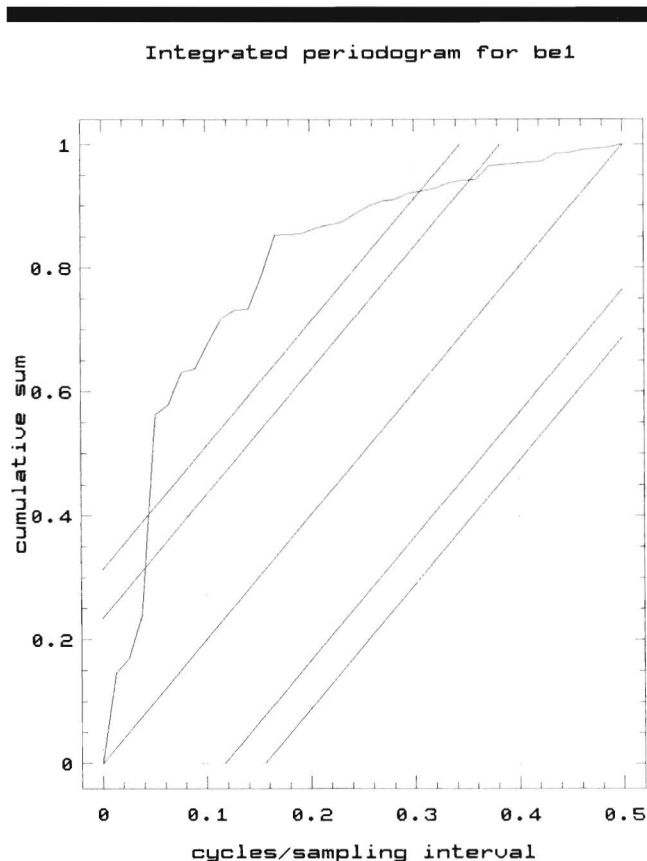


Figure 3. Integrated periodogram of the Kolmogorov-Smirnov test. Frequencies between 0.04–0.3 cycles/2ka are significant to >95%.

the observed record. Algorithms for MESA were derived from BURG (1967) and SMYLLIE, *et al.* (1973). Because of the inconclusive performance of the autoregressive order (F, Filters) we consider it necessary to implement three means of establishing the sufficient order of AR process. Such means can be the direct comparisons of MESA and FFT power spectra. The three criteria are: i) AKAIKE'S (1969) final prediction error (FPE); this exhibits the expected monotonically decreasing character as a function of the order of AR filter, ii) BERRYMAN'S (1978) criterion, where  $F = 2N/\ln 2N$ ,  $N =$  number of data, and iii) ULRYCH and BISHOP'S (1975) criterion, where  $N/3 < F < N/2$ .

Both the autocovariance (MESA) and FFT methods are "data adaptive" methods; that is, they see the data through a preselected fixed window and require the unrealistic assumption of a periodic or a small extension outside the observed record. Hence, the possibility of poor resolution and shifts in the spectrum peaks exists when the methods are for "short" data sequences, as in the present work.

The PSA power (variance) spectra (BLACKMAN and TUKEY, 1959) were obtained from autocorrelation functions which were truncated at various lags. Moreover, if the spectrum represents a random sample from a normal population, the sample spectrum estimates at a given frequency are distributed about the corresponding population spectrum according

to a chi-square distribution divided by the equivalent degrees of freedom. Therefore, the spectrum peaks are attached significance levels at 1%, 5% and 10%, for respective ratios of peaks-to-continuum.

The simultaneous application of these four complementary methods offers a check upon computational accuracy and stability, frequency and power spectral density, and allows a careful scrutiny of the periods of interest, and a reasonable determination of the actual periods present (LIRITZIS, 1990; XANTHAKIS and LIRITZIS, 1991).

The raw data were equally spaced per 2 ka fixed windows ( $N = 78$ ). Eleven such windows of 2 ka were missing and replaced with interpolated values. Subsequently this time-series was detrended by subtracting a 1st and then a 2nd order polynomial (Figure 1). Also, it was smoothed with a 3-terms moving average. In all the three smoothings/detrendings the obtained periodicities were almost similar and significant to >95%, as evidenced from the Kolmogorov-Smirnov cumulative periodogram. The randomness test, where the two-tailed probability of equaling or exceeding  $Z \ll 0.05$ , confirmed the nonrandom variation to the time-series. The periodicities obtained from the four methods of spectrum analysis are discussed below.

FFT and PSA: The FFT was applied to the whole detrended series as well as to sub-sets. The truncated records were

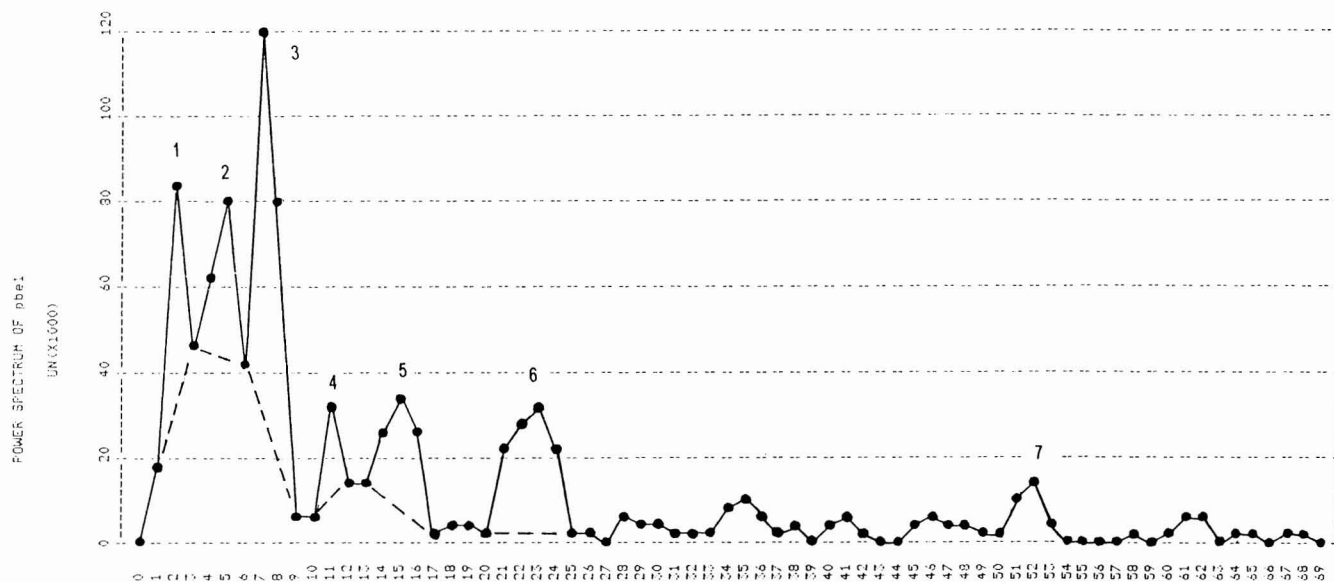


Figure 4. PSA spectrum for lag = 70. The dashed line defines the continuum. The ratio ( $r$ ) of peak-to-continuum determines the significance with Chi-square statistic. It is  $r = 4.605, 2.996$  and  $2.302$  for significance levels at 1%, 5% and 10% respectively.

made first by truncating the older data down to the first half, then truncating the recent data down to half of the second older half of the whole record. This was made to test the stationarity of  $^{10}\text{Be}$  time-series. The PSA was applied to the detrended record.

Significant variance (significance >95%) was observed for frequencies  $\sim 0.04\text{--}0.3$  cycles/2 ka, outside this band the significance was <95% (Figures 2,3). Attached errors in frequency peaks refer to their respective full width half maximum (FWHM).

Six periodic terms were obtained from the FFT, which on average for all subsets were:  $126.2 \pm 41.3$  ka,  $38.3 \pm 2.9$  ka,  $24.4 \pm 2.5$  ka,  $18.1 \pm 1.1$  ka,  $12.6 \pm 0.9$  ka and  $5.4 \pm 0.1$  ka. The PSA gave the following, almost similar results:  $140 \pm 40$  ka (80–85%),  $56 \pm 14$  ka (<80%),  $40 \pm 6$  ka (90–95%),  $25.4 \pm 2$  ka (80–85%),  $18.6 \pm 1.4$  ka (90–95%),  $12.2 \pm 1$  ka (99%) and  $5.4 \pm 0.3$  ka (99%) (Figure 4). The  $56 \pm 14$  ka peak is of low significance and rather represents side lobe of the high peak, a product of the method, for the period of the length of the record.

The  $126.2 \pm 41.3$  ka and  $140 \pm 40$  ka, exhibit a large fluctuation due to short length of the record. The  $38.3 \pm 2.9$  ka (or the  $40 \pm 6$  ka of the PSA) is present in most subsets and in the three detrending procedures, but absent in some subsets because, i) there its spectral power is being overdrawn by the higher period, ii) due to the short length of respective subsets (less than 75 ka), iii) the fact that FFT prefers the high length of the record as the highest period with sub-harmonics, and finally iv) from the need of tapering the ends of some subsets- as was proved for 10% or 20% data at both ends of the subset tapered with cosine bell- in addition to some effect from the interpolated values. However, the two

halves contain this period at the expense of the side lobes of the 126 and 25 ka periodicities (Table 1).

The  $24.4 \pm 2.5$  ka (or  $25.4 \pm 2$  ka in PSA) is present in the whole record and all subsets. Similarly, the  $18.1 \pm 1.1$  ka,  $12.6 \pm 0.9$  ka, and  $5.4 \pm 0.1$  ka, for FFT, which correspond to  $18.6 \pm 1.4$ ,  $12.2 \pm 1$  and  $5.4 \pm 0.3$  ka of PSA. The last one, as expected, is not present in the smoothed with 3-terms moving average record; its variance is low and lies near the Nyquist frequency ( $f_N = \frac{1}{2}\Delta t$ ,  $\Delta t = 2$  ka) corresponding to the period of 4 ka.

The  $\sim 20$  ka periodicity was also obtained from the cycling variation of the autocorrelation coefficients.

MESA: Similar treatment to FFT analysis gave similar periodicities to FFT and PSA except of the two around 20 ka, which here appear as one, the  $19.6 \pm 1.9$  ka. It is present in all subsets but with low variance. The high periodic term of  $107.8 \pm 33.7$  ka is present in all analyses, except of the short subsets, with large expected fluctuation (Figure 5).

The  $45.7 \pm 5.4$  ka appears in all subsets with a pronouncedly large variance. The  $12.9 \pm 1.3$  and  $5.4 \pm 0.03$  ka are also present but with a small variance in all subsets. The  $8 \pm 0.04$  ka period must be a by-product of the two periods 19.6 ka and 12.8 ka; according to the theory of combining sinusoids the 7.8 ka is obtained. This new period emerges in MESA which uses the maximum information from within the analyzed record ignoring extrapolations outside this length of data.

Varying the filter length ( $F = 10\text{--}70$ ), it was noticed the stability of the  $\sim 40$  ka,  $\sim 21$  ka, 12.5 and 5.4 ka periods for  $F = 20\text{--}45$ , with large variance taken mainly by the  $\sim 40$  and  $\sim 21$  ka peaks. Lower ( $F$ ) gives an oversmoothed spectrum with lost resolution, while for higher ( $F$ ), frequency splitting

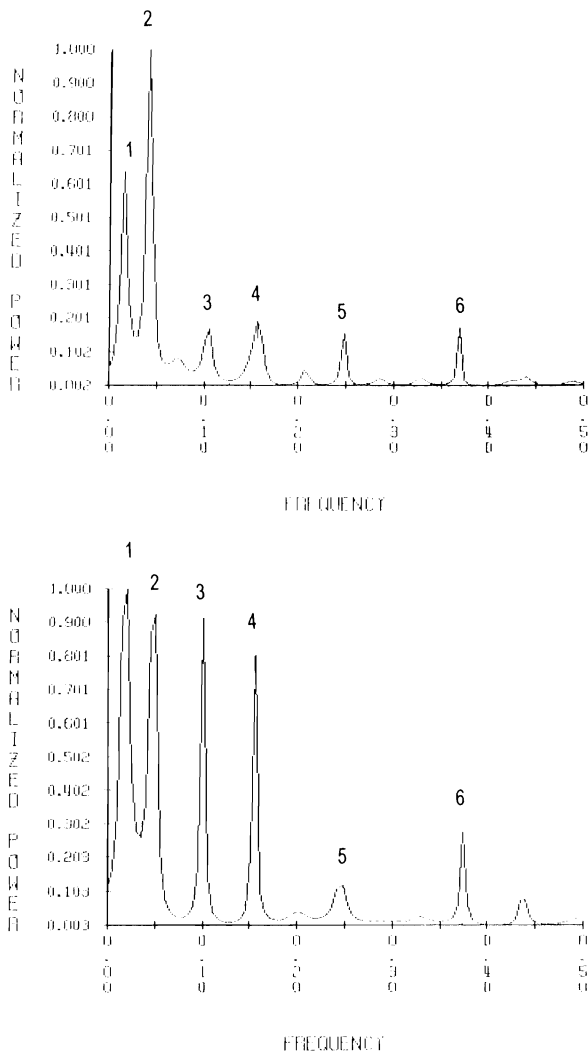


Figure 5. MESA spectra for, a) all the record ( $F = 31$ ), and b) for the subset 2-108 ka ( $F = 23$ ). Note the six periodicities presented in detail in Table 1.

and simultaneous splitting of the spectrum peaks occurs, giving a false spiky appearance to the spectrum.

The coefficients of the estimated autocorrelations for lags 40 ka followed a prominent cyclic pattern of  $\sim 20$  ka.

Similar results were obtained with the removal of two extreme spiky values from the analyzed time-series, and replaced by averages of adjacent data points. This implies that some anomalously high concentrations of  $^{10}\text{Be}$  in Antarctic ice cores (uncorrelated with  $\delta^{18}\text{O}$ ) overlap the regular variation of astronomical forcing, and sways opinion towards a stochastic process for their origin (from cosmic ray acceleration in propagating interstellar shock waves, which envelop the heliosphere and whose source may be ancient supernovas (SONETT *et al.*, 1987), or as due to magnetic "excursions" *i.e.* periods during which the apparent dipole direction and/or intensity at a given latitude fluctuate strongly from their "nor-

mal" values for periods of a few hundred to a few thousand years) (RAISBECK *et al.*, 1987; VEROSUB and BENERJEE, 1977).

However, the periodicities obtained from all spectral methods form a "network" of periodicities superimposed upon each other.

## DISCUSSION

The revealed periodicities, stationary and significant, under the present conditions of the data quality (measurement errors, missing values, length of record), are similar, with an apparent coincident anticorrelation, with the set of astronomical ones of the Milankovich insolation theory *i.e.* the fundamental periods of the planetary system, referred to the earth's orbit and rotation, that is the eccentricity, precession and obliquity (BERGER and PESTIAUX, 1984; BERGER, 1978). However, beside the Milankovich forcing, the additional peaks seem to correspond to major planetary motions (FAIRBRIDGE and SANDERS, 1987).

These astronomical elements have several components in their expansion, which have been found in several other geological, astronomical and geophysical spectra (XANTHAKIS *et al.*, 1995; BERGER, 1989; BERGER and PESTIAUX, 1984; BERGER, 1977, 1978, 1984; BERGER and LOUTRE, 1991).

The most important terms in eccentricity series expansion are; 413 ka, 95 ka, 136 ka. The last two contribute to a peak which is often loosely referred to as the 100 ka eccentricity cycle. Secondary peaks appear at 130 ka, 600 ka, 1.3 Ma, and 2.3 Ma. The four main terms in the expansion of precession have periods of 23.7 ka, 18.98 ka, 19.16 ka. In low resolution geological spectra these are seen as a single peak near the mean of 21 ka or as two peaks of 23 and 19 ka. The latter was observed with the FFT analysis. Secondary peaks appear at 15 ka, 17 ka and 56 ka. The Obliquity of 41 ka has secondary peaks at 30 ka and 53 ka. Some of these secondary coincide with those found in our analysis, though it is not clear if they are an artifact of the methods, secondary components, or major planetary motions.

It has been demonstrated (HAYS *et al.*, 1976) that the astronomical frequencies were significantly present in palaeoclimatic data; the 100-, 41-, 23-, and 19-Ka periods are superimposed on a general red noise spectrum.

A noteworthy spectrum analysis of lake sediment radioactivity has revealed several whole or quasiperiodicities ranging from 1 to 24 ka, the latter long period attributed to the precessional signal (XANTHAKIS *et al.*, 1992).

Regarding solar-planetary effects, the obtained periodicities, together with expected higher ones as well as the Milankovich cycles, coincide with planetary resonances. Thus, for example, the 5.3–5.6 ka periodicity seems to be the resonance cycle of 5.56 ka from: Solar Orbital Progression (SOP) of  $178.731 \text{ years} \times 31$ ; SJL (Saturn-Jupiter Lap) of  $19.8793 \text{ years} \times 280$ ; Solar Sunspot Cycle (SSC) of  $11.1212 \text{ years} \times 500$  (Note: these are mean values and each period is slightly variable). The 12–13 ka periodicity seems to have the same components to give a resonance of 12.5 ka, thus  $178.731 \text{ SOP} \times 70$ ;  $11.1212 \text{ SSC} \times 1124$ . The Planetary-Solar Quadrature Cycle (PSQC) of  $1112.1212 \text{ years} (556.06 \text{ years} \times 2; \text{SSC} \times$

Table 1. Periodicities with associated errors, where appropriate, of the respective spectral peaks of  $^{10}\text{Be}$ , per method of analysis, ordered sub-records, and various orders of autoregressive process (filters).

1a) MESA OF TOTAL RECORD AND VARIOUS FILTERS									
Filters			Periodicities (in ka)						
10	—	52.6	—	—	14.5	—	—	—	5.2
20	—	54	21.7	—	—	12.5	—	—	5.4
30	120	44	—	19	—	12.5	8	—	5.4
40	133	44	25	19	—	—	—	—	—
50	200	44.4	—	—	—	—	—	—	—
60	200	44.4	—	—	—	—	8	—	—
70	200	44.4	—	—	—	—	—	—	—
Average, F = 20–45 (persistent periods)		44	21	—	—	12.5	—	—	5.3
1b) MESA OF SUB-RECORDS									
		No. of Peak and Periodicities (ka)							
Interval (ka)	Filter	1	2	3	4	5	6		
1-155	31	120 ± 15	44.2 ± 4	19 ± 1	12.5 ± 0.2	8 ± 0.1	5.4 ± 0.1		
1-151	30	105 ± 21	46.7 ± 6	19 ± 3	12.9 ± 0.3	8 ± 0.1	5.4 ± 0.1		
1-147	30	105 ± 21	46.7 ± 6	19.2 ± 2	12.5 ± 0.4	7.9 ± 0.1	5.4 ± 0.1		
1-143	29	105 ± 21	52.5 ± 8.5	19.2 ± 1	12.5 ± 0.3	—	5.4 ± 0.1		
1-139	28	76.4 ± 20	44.2 ± 7	19.5 ± 1.3	12.5 ± 0.2	8 ± 0.1	—		
1-135	28	93.3 ± 28	44.2 ± 7	18.7 ± 1	12.5 ± 0.2	7.9 ± 0.15	—		
1-131	27	84 ± 24	42 ± 4	18.7 ± 1.2	12.5 ± 0.3	7.9 ± 0.1	—		
1-127	26	105 ± 35	42 ± 4	19.5 ± 1.3	12.5 ± 0.3	8 ± 0.15	—		
1-123	26	105 ± 35	42 ± 5	19.5 ± 1.3	12.3 ± 0.8	8 ± 0.1	—		
1-119	24	84 ± 24	38.2 ± 4	19.5 ± 1	12.3 ± 0.7	—	5.3 ± 0.1		
1-107	23	84 ± 14	38.1 ± 3.2	19 ± 0.6	12.7 ± 0.3	—	5.3 ± 0.1		
1-99	22	93.3 ± 28	44.2 ± 9	19 ± 0.9	12.7 ± 0.3	—	—		
1-91	20	—	49.4 ± 11	19.5 ± 1.6	12.7 ± 0.4	—	—		
1-83	19	—	52.5 ± 13	—	12.5 ± 0.6	—	—		
1-75	17	—	52.5 ± 20	—	12 ± 0.6	—	—		
5-155	30	140 ± 35	42 ± 5	19 ± 0.9	12.7 ± 0.3	—	5.4 ± 0.06		
7-155	30	210 ± 70	42 ± 4	18.2 ± 0.7	12.7 ± 0.4	7.9 ± 0.1	5.3 ± 0.1		
13-155	29	—	38.2 ± 8	—	13.1 ± 0.5	—	5.3 ± 0.05		
17-155	28	—	38.1 ± 4	19 ± 1.6	12.7 ± 0.4	—	—		
21-155	28	—	38.1 ± 11	19 ± 1.6	12.5 ± 0.3	—	—		
25-155	27	—	38.2 ± 7	18.7 ± 1	—	—	—		
33-155	26	—	35 ± 6	—	12.7 ± 0.6	—	—		
41-155	24	—	46.7 ± 5	—	—	—	—		
49-155	23	—	46.7 ± 5	—	—	—	—		
57-155	22	—	46.7 ± 7	—	—	—	—		
65-155	20	—	49.4 ± 10	26.2 ± 2	—	—	—		
75-155	19	52.5 ± 20	38.2 ± 7	—	—	—	—		
Average		107.8 ± 33.7	43.6 ± 5.3	19.6 ± 1.9	12.9 ± 1.3	7.9 ± 0.05	5.4 ± 0.04		

From the absent peaks, most appear with very low power and omitted, while the absent ones reappear when the analysed sub-record is tapered at the end. The uncertainty of the average is the standard error of the mean

100) is plotted on the harmonic/cyclic graph herewith (Figure 6). It identifies both the principal mean Milankovich periods and the Be-10 spectral peaks, with a fair degree of precision. The Be-10 spectra higher than 95 ka are explained as “projected” possibilities. The obtained periods are bound into the less than  $10^3$  cycles part of the abscissa.

The many common periodicities found in several solar-terrestrial phenomena (e.g. sunspots, C-14, geomagnetic intensity, tree-rings, terrestrial landforms and deposits,  $^{10}\text{Be}$  and  $^{18}\text{O}$  in polar ice, and even thermoluminescence signal in marine sediments) may offer interpretation for the possible causes of climate changes, considering mainly the potential impact of a past and present variable sun, which exhibits long (>1 ka) and short-term periodicities, coupled with earth's orbital and geomagnetic changes.

It would be interesting to carry out similar analyses to oth-

er  $^{10}\text{Be}$  long records from other latitudes to examine the effect of each astronomical forcing to the  $^{10}\text{Be}$  variation.

The physical/geophysical mechanism pertinent to the variation of  $^{10}\text{Be}$  in polar ice due to the astronomical forcing must be sought in the manner the  $^{10}\text{Be}$  is produced, the rate of production and its transportation-deposition down to earth.

Potential sources of  $^{10}\text{Be}$  production/deposition rate are: i) variation in primary cosmic-ray flux, ii) changes in solar modulation, iii) changes in geomagnetic field intensity, iv) circulation pattern in the atmosphere. The long-term modulation of (ii) and (iii) is probably related to the obtained periodicities in the ka range.

However, as the  $^{10}\text{Be}$  variation correlates with  $\delta^{18}\text{O}$  (RAISBECK *et al.*, 1987; DANSGAARD *et al.*, 1993)—high temperature, low  $^{10}\text{Be}$ —the temperature is considered as the dominant factor in precipitation rate. Theoretical estimations have

Table 1. *Continued*

Interval (ka)	No. of Peak and Periodicities (ka)					
	1	2	3	4	5	6
1-155	131 ± 32	38 ± 3.5	26.2 ± 2.5	18.4 ± 2.3	12.5 ± 0.9	5.4 ± 0.1
1-151	147.5 ± 50	40.6 ± 5	26.2 ± 2	18.4 ± 2.4	12.5 ± 0.9	5.4 ± 0.1
1-147	131 ± 52	34.7 ± 4	24.6 ± 3	18.4 ± 1.1	12.3 ± 0.9	5.4 ± 0.1
1-143	147.5 ± 78	34.7 ± 5	21.8 ± 3	17.9 ± 1.3	12.4 ± 1	5.4 ± 0.1
1-139	118 ± 55	34.7 ± 5	20 ± 3	—	12.5 ± 1	5.4 ± 0.1
1-135	118 ± 64	39.3 ± 12	—	19.3 ± 1.5	12.4 ± 0.6	5.4 ± 0.1
1-131	147 ± 100	—	—	18.7 ± 1.4	11.9 ± 1	5.3 ± 0.2
1-127	—	33.8 ± 4	—	19.2 ± 1.5	13 ± 1	5.3 ± 0.1
1-123	73.5 ± 28	39.3 ± 6	24.6 ± 3.5	17.6 ± 1.3	12.3 ± 0.5	5.4 ± 0.1
1-119	158.7 ± 77	36.8 ± 7	—	19 ± 2	12.8 ± 1	5.3 ± 0.1
1-107	111 ± 50	38 ± 8.5	—	17.9 ± 1.8	12.1 ± 0.7	5.4 ± 0.1
1-99	98.3 ± 40	35.7 ± 6	—	20.3 ± 2.5	12.7 ± 1.4	—
1-91	84.3 ± 46	—	—	18.1 ± 2	13.1 ± 1.2	5.4 ± 0.1
1-83	59 ± 25.3	—	—	18.7 ± 2	12 ± 0.7	5.3 ± 0.2
1-75	—	40.7 ± 9	—	18.7 ± 2.5	12.5 ± 0.5	5.4 ± 0.3
5-155	168.6 ± 40	40.7 ± 7	25.6 ± 2	19 ± 1.2	11.8 ± 0.5	5.4 ± 0.1
7-155	196.6 ± 98	39.3 ± 5	—	18.4 ± 1.3	13.4 ± 1	5.4 ± 0.2
13-155	147.5 ± 63	38 ± 4	—	18.1 ± 1.3	13.3 ± 0.9	5.3 ± 0.1
17-155	168.6 ± 60	33.7 ± 6	—	17.9 ± 1.5	12.3 ± 1	5.4 ± 0.1
21-155	118 ± 60	—	28 ± 4	—	14.2 ± 1.5	5.5 ± 0.1
25-155	200 ± 100	—	26.2 ± 5	18.7 ± 0.5	12.5 ± 1.3	5.5 ± 0.2
33-155	147 ± 56	39.3 ± 5	24.5 ± 3.5	17.6 ± 2	11.9 ± 1	5.4 ± 0.1
41-155	118 ± 52	36.8 ± 8	25.6 ± 5	15.1 ± 3	11.5 ± 0.6	5.5 ± 0.1
49-155	54 ± 26	—	—	18.1 ± 1.6	13.4 ± 1.3	5.4 ± 0.1
57-155	59 ± 19	—	26.2 ± 3	—	15.5 ± 2.5	5.5 ± 0.1
65-155	—	40.7 ± 6	22.6 ± 3.5	—	11.5 ± 0.7	5.4 ± 0.2
73-155	—	45.4 ± 16	—	15.3 ± 2.5	—	5.6 ± 0.2

Broad peaks appear at shorter subsets, associated with large uncertainties

## 3) PSA

Interval (ka)	No. of Peaks and Periodicities (ka)	χ <sup>2</sup> -test Significance
1-155	1	140 ± 40
	2	56 ± 14
	3	40 ± 6
	4	25.4 ± 2
	5	18.6 ± 1.4
	6	12.2 ± 1
	7	5.4 ± 0.3

shown that for the Antarctica plateau (YIYOU *et al.*, 1985); while simulation (HAYS *et al.*, 1976) from a regressive model, using the insulations as a forcing (BERGER, 1988), gave a best fit to the measured δ<sup>18</sup>O. Taking into account the above and the, already noted, anticorrelation between eccentricity-obliquity-precession combined long-term variation curve and <sup>10</sup>Be concentration curve, these factors reestablish the astronomical forcing of the already found periodicities for <sup>10</sup>Be. We should note that in the <sup>10</sup>Be concentration records, the dominant signal with an amplitude of a factor 2–3 is the accumulation rate, which is highly correlated with the <sup>18</sup>O signal (DANSGAARD *et al.*, 1993).

Apart of the variation of large-scale circulation which is the principal variation due to temperature distribution, further effects pertinent to <sup>10</sup>Be regular, but also superposed irregular, fluctuations can be invoked from by-products of temperature variation, such as, the moisture input, latent heat, shifts of mass in the atmosphere, development of surface wind and weather systems, cloud development and weather, cyclogenesis, general distribution of wind zones (*e.g.* wester-

lies). Also in Antarctica, late winter brings the most disturbed regime and any wind exceeding 5–7 m/sec may upset the light powdery surface snow drifting it. Last, other agents affecting wind circulation may be volcanic aerosols, which may cause sudden season changes (see also, LAL, 1987).

Therefore, the earth's orbit and rotation causes changes, a) in the earth-sun distance and thus temperature, and b) in the impinging angle of cosmic-rays on the magnetosphere, which coupled with the changes in geomagnetic secular (dipolar) and non-dipole field, results to a latitudinal gradient in the <sup>10</sup>Be variation.

All the above determine the <sup>10</sup>Be concentration, rate of production and precipitation. We believe that the <sup>10</sup>Be concentration variation in the Antarctic ice cores is caused from the above two factors which are driven by the astronomical forcing. Exceptional values present as outliers are due to rather randomly varying agents *e.g.* extraterrestrial shock waves, anomalous and sudden wind circulation changes, volcanic eruptions, sudden infrequent solar activity emissions.

The apparent network of periodicities found here for the



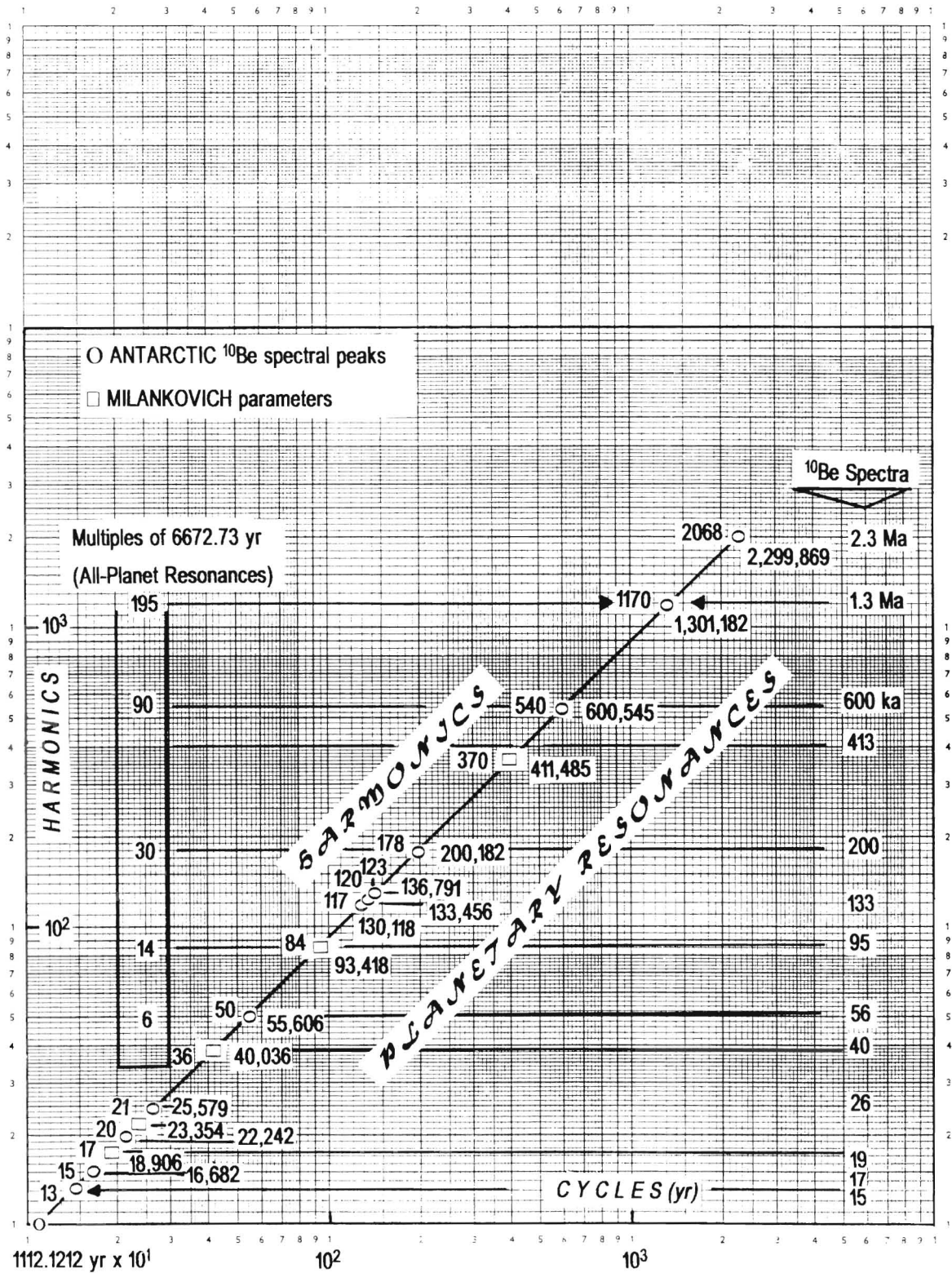


Figure 6. Harmonics of All-Planet Resonances, against, Cyclicity of Planetary-Solar Quadrature Cycle of 1.1121212 ka (= 100 × sunspot cycle of 11.1212 yrs). Harmonic scale (left) is in orders of magnitude (× 1112 yr), and Cycle scale (abscissa) are also orders of magnitude (numbers of cycles). Diagonal line determined from multiples of 1112 yr, which closely correspond to Milankovich values of Earth/Moon/Sun orbital variables, e.g. the elliptic cycle approx. 40,036 yr = 36 × 1112 (or 3600 times the sunspot cycle mean). The 93,418 yr (= 84 × 1112.12) is the eccentricity cycle, which has several values,



$^{10}\text{Be}$  concentration and elsewhere, reinforces the complicated behaviour of dynamical (orbital, pulsed forcing) solar-planetary system, combined with the self-organization of earth's response. (XANTHAKIS *et al.*, 1992; LIRITZIS and GALLOWAY, 1995; RAMPINO *et al.*, 1987).

### CONCLUSION

The  $^{10}\text{Be}$  concentrations in the east Antarctic ice (Vostok and Dome C coastal sites) have been spectrally analysed and significant periodicities similar to the well known astronomical frequencies were disclosed. That is, the long-term variations in the geometry of the earth's orbit around the sun and rotation, as the fundamental causes of Pleistocene ice-ages of the past 3 Ma. This variation along with the production mechanism of  $^{10}\text{Be}$  and its deposition onto ice-caps is linked with  $\delta^{18}\text{O}$  and temperature trends, as well as short and long-term solar and geomagnetic variation.

Such analysis provides important clues regarding palaeoclimate reconstruction in polar regions, sea-level fluctuations, and especially possible relationships between several solar, terrestrial and planetary agents.

### ACKNOWLEDGEMENTS

This is an ongoing project of the Academy of Athens, IL thanks Fyrogenis SA for partial support. We are thankful to Prof. R. Fairbridge for constructive comments and for suggesting Figure 6, and Prof. P. Ligomenidis for his kindness to facilitate the execution of this work.

### LITERATURE CITED

- AKAIKE, H., 1969. Power spectrum estimation through autoregressive model fitting. *Annals Institute Statistics Math*, 21, 243–247.
- BERGER, A., 1977. Support for the astronomical theory of climatic change. *Nature*, 269, 44–45.
- BERGER, A., 1978. Long-term variations of caloric insolation resulting from the earth's orbital elements. *Quaternary Research*, 9, 139–167.
- BERGER, A., 1984. Accuracy and frequency stability of the earth's orbital elements during the quaternary. In: BERGER, A.L. *et al.*, (eds), *Milankovich and Climate*, Dordrecht: Reidel Part I, 3–39 pp.
- BERGER, A., 1989. Pleistocene climatic variability at astronomical frequencies. *Quaternary International* 2, 1–14.
- BERGER, A., 1988. Milankovich theory and climate. *Reviews Geophysics*, 26(4), 624–657.
- BERGER, A. and PESTIAUX, P., 1984. Modelling the astronomical theory of palaeoclimates in the time and frequency domain. In: GHASI, A. and FANTECHI, R. (eds), *Current Issues of Climate Research*, Dordrecht; Reidel pp. 77–96.
- BERGER, A. and LOUTRE, M.F., 1991. Insolation values for the climate of the last 10 million years. *Quaternary Science Reviews*, 10, 297–317.
- BERRYMAN, J.G., 1978. Choice of operator length for maximum entropy spectral analysis. *Geophysics*, 43, 1383–1391.
- BLACKMAN, R.G. and TUKEY, J.W., 1959. *The Measurement of Power Spectra from the Point of View of Communications Engineering*. New York: Dover.
- BOWEN, R., 1991. *Isotopes and Climates*. London: Elsevier, 483p.

- BURG, G.P., 1967. Maximum entropy spectral analysis. In: *37th Annual International Meeting Society Exploration Geophysics* (Oklahoma City).
- CHATFIELD, C., 1984. *The Analysis of Time-Series*. London: Chapman and Hall, 286.
- DANSGAARD *et al.*, 1993. *Nature*, 364, 218–220.
- HAYS, J.D.; IMBRIE, J., and SHACKLETON, N.J., 1976. Variations in the Earth's orbit: Pacemaker of the ice ages. *Science*, 194, 1121–1132.
- LAL, D. and PETERS, B., 1967. Cosmic-ray produced radioactivity on the earth. In: *Handbook of Physics*, vol. 46/2, pp. 551–612 (Springer-Verlag, Berlin).
- LAL, D., 1987.  $^{10}\text{Be}$  in polar ice data reflect changes in cosmic ray flux or polar meteorology. *Geophysical Research Letters*, 14, 785–788.
- LIRITZIS, I. Evidence for periodicities in the auroral occurrence frequency since 300 A.D. and their implications. *Pure & Applied Geophysics*, 133(2), 201–211.
- LIRITZIS, I.; PETROPOULOS, B.; XANTHAKIS, J.; BANOS, C., and SARRIS, E., 1995. Detailed spectral analysis of Jupiter's Great Red Spot: relative intensities for the period 1963–1967. *Planetary Space Science*, 43(9), 1967–1978.
- LIRITZIS, I. and GALLOWAY, R.B., 1995. Solar-Climatic effects on lake/marine sediment radioactivity variations. In: FINKL, C.W., (ed.), *Holocene Cycles, Climate, Sea Levels and Sedimentation*. Journal of Coastal Research, Special issue No 17, Ch. 10, Charlottesville, Virginia: Coastal Education and Research Foundation, pp. 63–71.
- LORIUS, C.; JOUZEL, J.; RITZ, L.; MERLIVAT, L.; BARKOV, N.I.; KOROTKEVICH, Y.S., and KOTLYAKOV, V.M., 1985. A 150,000-year climatic record from Antarctic ice. *Nature*, 316, 591–596.
- McHARGUE, L.R. and DAMON, P.E. 1991. The global beryllium-10 cycle. *Reviews Geophysics*, 29, 141–158.
- RAMPINO, M.R.; SANDERS, J.E.; NEWMAN, W.S., and KONIGSSON, L.K., 1987. *Climate: History, Periodicity and Predictability*. New York: Van Nostrand Reinhold.
- RAISBECK, G.M.; YIOU, F.; BOURLES, D.; LORIUS, C.; JOUZEL, J., and BARKOV, N.I., 1987. Evidence for two intervals of enhanced  $^{10}\text{Be}$  deposition in Antarctic ice during the last glacial period. *Nature*, 326, 273–277.
- RAISBECK, G.M.; YIOU, F.; FRUNEAU, M.; LOISEAUX, J.M.; LIEUVIN, J.C.; RAVEL, J.C., and LORIUS, C., 1981. Cosmogenic  $^{10}\text{Be}$  concentrations in Antarctic ice during the past 30,000 years. *Nature*, 292, 825–826.
- SMYLIE, J.E.; CLARK, G.K.C., and ULRICH, T.J., 1973. Analysis of irregularities in the earth's rotation. *Methods in Computational Physics*, pp. 391–430.
- SONETT, C.P.; MORFILL, G.E., and JOKIPIL, J.R., 1987. Interstellar shock waves and  $^{10}\text{Be}$  from ice cores. *Nature*, 330, 458–460.
- ULRYCH, T.T. and BISHOP, T.N., 1975. Maximum entropy spectral analysis and autoregressive decomposition. *Reviews Geophysical Space Physics*, 13, 183–200.
- VEROSUB, K.L. and BENERJEE, S.K., 1977. Geomagnetic excursions and their palaeomagnetic record. *Rev. Geophys. Space Phys.* 15, 145–155.
- XANTHAKIS, J.; LIRITZIS, I., and TZANIS, A., 1995. Periodic variation of  $\delta^{18}\text{O}$  from V28-239 Pacific ocean deep-sea core. *Earth, Moon, Planets*, 66, 253–278.
- XANTHAKIS, J.; LIRITZIS, I., and GALLOWAY, R.B., 1992. Periodic variation in natural radioactivity of lake Bouchet sediments. *Earth, Moon, Planets*, 59, 191–200.
- XANTHAKIS, J. and LIRITZIS, I., 1991. Geomagnetic field variation as inferred from archaeomagnetism in Greece and palaeomagnetism in British lake sediments since 7000 B.C. *Academy of Athens Publication* 53, 222 p.
- YIOU, F.; RAISBECK, G.M.; BOURLES, D.; LORIUS, C., and BARKOV, N.I., 1985.  $^{10}\text{Be}$  in ice at Vostok Antarctica during the last climatic cycle. *Nature*, 316, 616–617.

but this is the prominent. A similar cluster of terms ( $\sim 20$  ka) apply to the precession, ranging over 6 ka; typical example is the 23,354 yrs. Circles (○) are for Antarctic  $^{10}\text{Be}$  spectral peaks, presented from present analysis and calculated (expected) also, on the right ordinate, and squares (□) are the Milankovich parameters. The black-outlined column on left side are multiples of 6672.73 yr, which is  $6 \times 1112$  yr, and corresponds to an "All Planet Resonance".